Dalton Transactions

ROYAL SOCIETY OF CHEMISTRY

PAPER

View Article Online
View Journal | View Issue

Cite this: *Dalton Trans.*, 2026, **55**, 3388

Hybrid amino/iminopyridines with auxiliary phosphines enabling active zinc catalysts for the ring-opening polymerization of lactide

Xiaopan Xue,[a,b] Dongzhi Zhu,[b] Wenjuan Zhang, *[a] Tongxin Zheng,[a,b] Rui Wang,[a] Yanping Ma [b] and Wen-Hua Sun *[b]

The series of 2-(diphenylethyl)amino-6-iminopyridines, 2-((Ph$_2$PCH$_2$CH$_2$)N=CMe)-6-(ArN=CMe)C$_5$H$_3$N (Ar = 2,6-^{i}Pr$_2$C$_6$H$_3$ (**L1**), 2,6-Et$_2$C$_6$H$_3$ (**L2**), 2,6-Me$_2$C$_6$H$_3$ (**L3**), 2,4,6-Me$_3$C$_6$H$_2$ (**L4**), and 2,6-(CHPh$_2$)$_2$-4-MeC$_6$H$_2$ (**L5**)), and the analogue 2-(*n*-butyl)amino-6-iminopyridine **L6** were synthesized and used to form their dichlorozinc complexes, LZnCl$_2$ (**Zn1–Zn6**). All organic compounds and zinc complexes were well characterized by ^{1}H/^{13}C/^{31}P NMR spectroscopy and elemental analysis, along with single-crystal X-ray diffraction of **Zn1** and **Zn4**, indicating bistrigonal geometry around zinc. By treatment with two equivalents of LiN(SiMe$_3$)$_2$, **Zn1–Zn6** exhibited high activities toward the ring-opening polymerization (ROP) of L-lactide (L-LA), indicating the positive influence of the substituents as well as the auxiliary phosphine. Notably, excellent activity was achieved even at high temperature; for example, **Zn1**/2LiN(SiMe$_3$)$_2$ catalyzed 2000 equiv. L-LA with 86% conversion in 10 minutes at 100 °C, with a TOF of 10 320 h^{-1}. The observed activities with respect to substituents were isopropyl > ethyl > methyl; thus, higher activities were achieved for more alkyl substituents. The auxiliary phosphine enhanced the activities of the zinc complexes; **Zn1–Zn5** showed higher activities than **Zn6** (with butyl), which formed the PLA with a lower molecular weight. The coordination–insertion and ring-expansion mechanisms have been proposed for the ROP of L-lactide.

Received 29th November 2025,
Accepted 15th January 2026

DOI: 10.1039/d5dt02857d

rsc.li/dalton

Introduction

Polylactides (PLAs), as an important biorenewable and biodegradable aliphatic polyester, have garnered significant attention owing to their sustainable life cycle and low environmental footprint.[1] Especially, these materials have broad applications in areas such as packaging, textiles, and medical instruments. Usually, they were prepared *via* ring-opening polymerization (ROP) of lactides catalyzed by organometallic compounds, in which tin(II) octoate [Sn(Oct)$_2$] is predominantly used in in dustrious processes under solvent-free conditions at high temperatures (190–200 °C) due to its high catalytic efficiency, excellent monomer compatibility, and minimal racemization.[2–4] However, growing health concerns regarding the accumulation of tin residue in the final products have prompted urgent demands for alternative catalytic systems. In this context, zinc-based catalysts have emerged as a promising solution, capitalizing on zinc's inherent biocompatibility, cost-effectiveness, and synthetic versatility. The synergistic interaction between zinc's strong Lewis acidity and tunable coordination environment enables precise control of polymerization and topological architectures, positioning zinc compounds as promising catalysts for sustainable ring-opening polymerization (ROP) methodologies for biodegradable polymers.

To date, there have been many studies on zinc compounds for the ROP of cyclic esters. According to the chelating heteroatoms, such as O, N, S, P, and their different donor abilities, zinc compounds can be catalogued into oxygen-based and non-oxygen-based zinc complexes. Among oxygen-based zinc complexes, phenoxyl-based derivatives have mostly been employed for the preparation of zinc complexes with chelating models of N^O, N^N^O as well as N^N^N^O.[3,5,6] For instance, phenoxyimino-based tridentate **1** has shown moderate to high performance for the controlled polymerization of *rac*-LA and L-LA as well as the random copolymerization of L-LA and ε-CL.[7,8] Moreover, the linking group present between the two nitrogen atoms in **1**, as well as the co-ligand X, can also greatly influence their catalytic performance.[9,10] By comparison, the phenoxylamino-zinc complexes, **2**, appended with different nitrogen donors display good isoselectivities and high activi-

[a]*Beijing Key Laboratory of Clothing Materials R&D and Assessment, Beijing Engineering Research Center of Textile Nanofiber, School of Materials Design and Engineering, Beijing Institute of Fashion Technology, Beijing 100029, China. E-mail: zhangwj@bift.edu.cn*

[b]*Key Laboratory of Engineering Plastics and Beijing National Laboratory for Molecular Science, Institute of Chemistry, Chinese Academy of Sciences, Beijing 100190, China. E-mail: whsun@iccas.ac.cn*

ties (P_m up to 0.87 and TOF up to 3312 h^{-1} at 25 °C) for *rac*-LA polymerization.[11,12] The other claw-type aryloxide zinc complexes, **3**, have also been extensively investigated.[13] Beyond this, the β-ketoiminate-based zinc complexes, **4**, are also desirable and display low to high activity for ROP of L-LA; they also showed stereoselectivity for the ROP of *rac*-LA in some cases.[14–16]

In contrast, non-oxygen-donated zinc complexes are limited; of those few, the N^N bidentate and N^N^N tridentate zinc complexes were most studied (shown in Chart 1).[17] The bis(guanidine) stabilized zinc complexes **5**, representing bidentate complexes, not only exhibited high activity for ROP of lactides, but also showed the high robustness at high temperatures along with oxidation and residual protic impurities within the monomer under the industrially relevant conditions, being replacing $Sn(Oct)_2$.[18] The chiral N^N bidentate zinc complexes,**6–7** (Chart 1), showed stereoselectivity for ROP of *rac*-LA, as representative examples.[19–21] N^N^N-Bound zinc complexes, **8–13** (Chart 1), have also demonstrated aptitude for the ROP of cyclic esters. In particular, binuclear **8** has shown remarkable activities for the ROP of LA, with turnover frequencies (TOF) reaching up to 60 000 h^{-1}, much higher than that observed for the ROP of ε-CL and *rac*-LA by mononuclear quinoline-based **10**.[22,23] Zinc complexes bearing β-diketiminate ligands **9** exhibited excellent catalytic activity and high steric selectivity in catalysing the ROP of cyclic esters.[24]

A few tetradentate zinc complexes, chiral heteroscorpionate zinc complexes **14** (Chart 1),[25] have been shown to be promising for the preparation of highly isotactic stereoblock PLA, whilst their amidinate heteroscorpionate analogues are efficient for the ROP of ε-CL and L-LA. Alternatively, the tetradentate zinc complexes with sulphur **15** (Chart 1) were reported to have low activity.[26]

Briefly, most ligand frameworks used in zinc-mediated ROP are based on hard oxygen- or nitrogen-donors. Considering the Lewis acidity of the zinc(II) ion and its borderline hard/soft nature, the effect of a soft donor phosphine group on the polymerization process is worthy of investigation. The use of P-coordinated zinc complexes for the ROP of cyclic esters remains limited.[27] The first examples of a phosphine-containing P^N-zinc complex **16** (Chart 1) could initiate the ROP of ε-CL.[28] C^N^P -tridentate zinc **17** (Chart 1) and P^P^P-tridentate complex **18** (Chart 1) were reported to exhibit varied performance for the ROP of ε-CL.[29–31]

Previously, we developed a series of 2-amino-6-iminopyridines with a pendant phosphorous group, and described their ruthenium, zinc, and iron complexes, **19–21** (Chart 1), in which the ligands chelated to the core metal in tridentate or bidentate modes. Among them, the N^N bidentate zinc complex displayed good activity for ROP of lactides and ε-CL,[32–34] while the tridentate iron complexes showed high activity for ROP of ε-CL, producing high-molecular-weight polymers (M_n up to 24 × 10^4 g mol^{-1}).[32] Very recently, by using these iron complexes, the ring-opening polymerization and

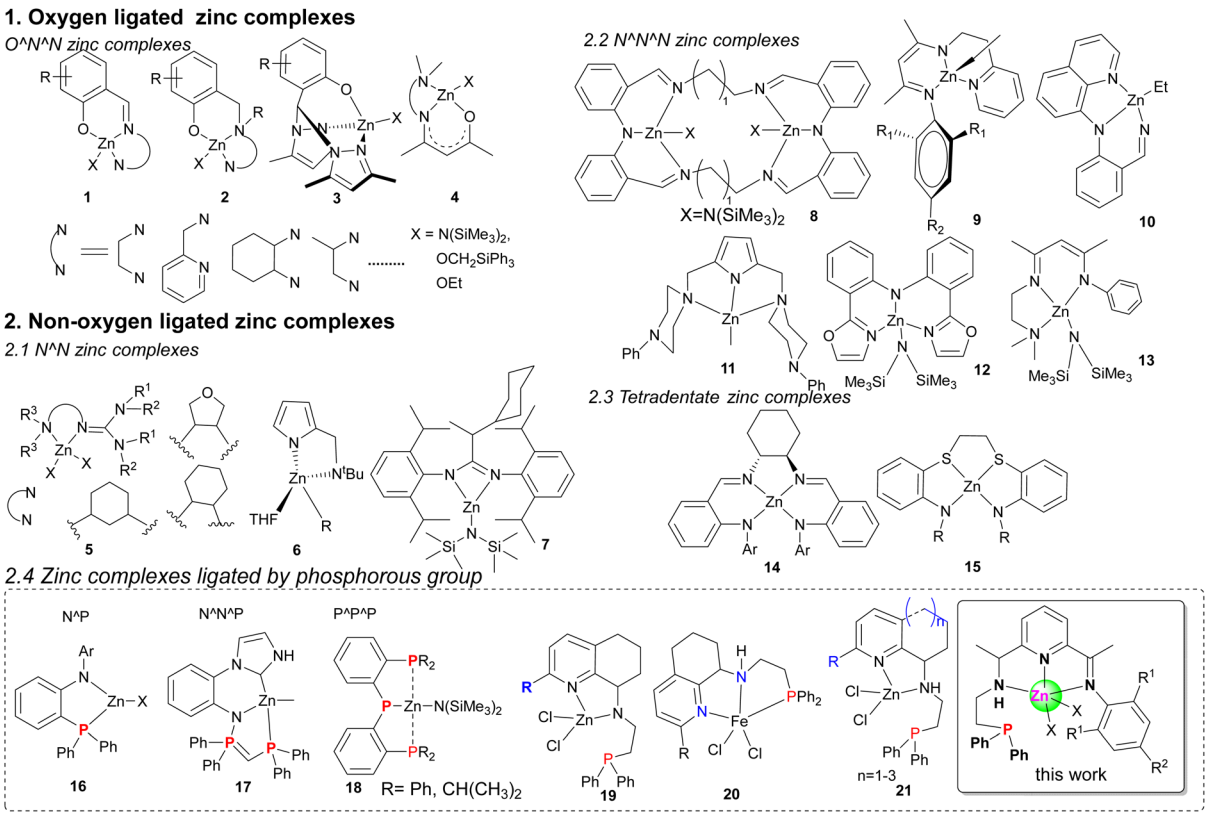

Chart 1 The representative zinc complexes for ROP of cyclic esters.

copolymerization of different lactides to produce random or block functional polylactides were achieved in our group.[35] However, the structural diversity was restricted by limited substituents on the pyridine moiety. Subsequently, the fused-cycloalkyl complexes were used to impose steric rigidity, hindering C–N bond rotation and further limiting conformational adaptability. Notably, the 2,6-bis(imino)pyridines, with easily varied steric bulk, were extensively explored for olefin polymerization;[36] however, the ability of their metal complexes to catalyze the ROP of cyclic esters has remained unclear. To explore the scope of catalysis, the pincer-type zinc complexes bearing 2-imino-6-aminopyridine with a pendant $-CH_2CH_2P(Ph)_2$ group were designed and evaluated for ROP of lactides in this work. The results showed that they displayed remarkable activity for the ROP of lactide, with catalytic performance critically dependent on substituent effects.

Results and discussion

Synthesis and characterization of L1–L5 and their zinc(II) complexes Zn1–Zn5

The five unsymmetrical 2,6-bis(arylimino)pyridines, 2-((Ph$_2$PCH$_2$CH$_2$)N═CMe)-6-(ArN═CMe)C$_5$H$_3$N (Ar = 2,6-^{i}Pr$_2$C$_6$H$_3$ (**L1**), 2,6-Et$_2$C$_6$H$_3$ (**L2**), 2,6-Me$_2$C$_6$H$_3$ (**L3**), 2,4,6-Me$_3$C$_6$H$_2$ (**L4**), and 2,6-(CHPh$_2$)$_2$-4-MeC$_6$H$_2$ (**L5**)), were prepared as shown in Scheme 1. Firstly, the imine-ketone intermediate, (*E*)-1-(6-(1-((aryl)imino)ethyl)pyridin-2-yl)ethan-1-one (aryl = 2,6-^{i}Pr$_2$C$_6$H$_3$, 2,6-Et$_2$C$_6$H$_3$, 2,6-Me$_2$C$_6$H$_3$, 2,4,6-Me$_3$C$_6$H$_2$, 2,6-(CHPh$_2$)$_2$-4-MeC$_6$H$_2$), was synthesized by reacting 2,6-diacetylpyridine with the corresponding aniline using approaches described previously (^{1}H NMR spectrum shown in Fig. S1–S6).[32] Secondly, by a similar method,[32] treatment of the respective imine-ketone with Ph$_2$PCH$_2$CH$_2$NH$_2$ in 1,2-dichloroethane (DCE), with NaBH(OAc)$_3$ employed as reduction reagent, afforded **L1–L5**. The zinc complexes **Zn1–Zn5** could then be smoothly prepared by treatment of **L1–L5** with zinc(II) chloride in ethanol at room temperature (Scheme 1). Both **L1–L5** and their respective zinc complexes **Zn1–Zn5** were characterized by ^{1}H/^{13}C/^{31}P NMR spectroscopy as well as elemental analysis. On comparison of the ^{1}H and ^{13}C NMR spectra of **Zn1–Zn5** with those of the free ligands **L1–L5** (shown in Fig. S7–S38), clear differences in the chemical shift were observed, in line with coordination having taken place. On the other hand, their ^{31}P NMR spectra showed singlet resonances in the range δ 20.94 to 21.69 ppm, with relatively little variation in chemical shift when compared with that of **L1–L5** (δ 21.31 to 21.46 ppm, see Table SI-1), which indicated that the phosphine remained pendant in solution, as seen in the solid-state structure. A similar observation, that phosphine donors in multidentate ligands (*e.g.*, pincer ligands) have the potential to dissociate with zinc in solution, has been reported.[32]

In addition, the molecular structures of **Zn1** and **Zn4** were further determined by single-crystal X-ray diffraction studies. Single crystals of **Zn1** and **Zn4** for X-ray determination were obtained by diffusing diethyl ether into their dimethylacetamide solution at room temperature; their structures are shown in Fig. 1 and 2, respectively. Selected bond lengths and angles are collected in Table 1. The crystal structures showed that they were very similar. In both cases, zinc was coordinated by three nitrogens and two chlorides, with a trigonal bipyramidal geometry around zinc. The coordination plane of the three nitrogens is almost coplanar with pyridine, and the aryl plane is almost perpendicular to the coordination plane, with a dihedral angle of 87.97° in **Zn1** and 87.42° in **Zn4**.

In addition, the bond length of Zn–N$_{py}$ is much shorter than those of Zn–N$_{amine}$ and Zn–N$_{imine}$ in both cases [2.069(3) Å *vs.* 2.282(4) Å, 2.325(3) Å in **Zn1**, 2.069(2) Å *vs.* 2.219(2) Å, 2.352(2) Å in **Zn4**], indicating the stronger coordination ability

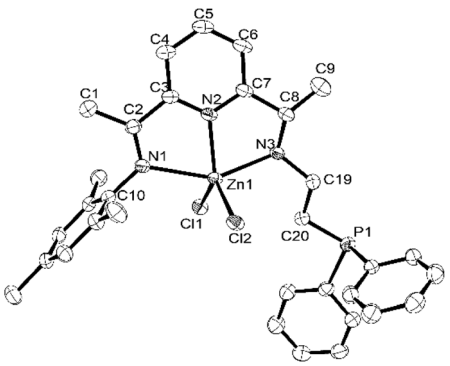

Fig. 1 ORTEP diagram of **Zn1** with the thermal ellipsoids set at the 30% probability level. Hydrogen atoms have been omitted for clarity.

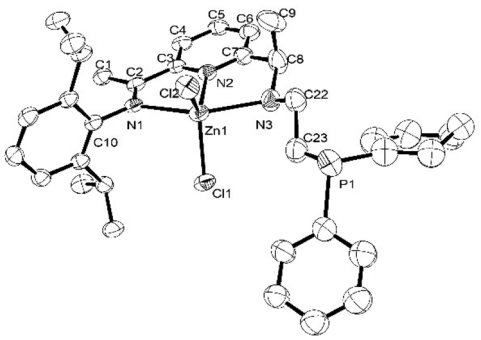

Fig. 2 ORTEP diagram of **Zn4** with the thermal ellipsoids set at the 30% probability level. Hydrogen atoms have been omitted for clarity.

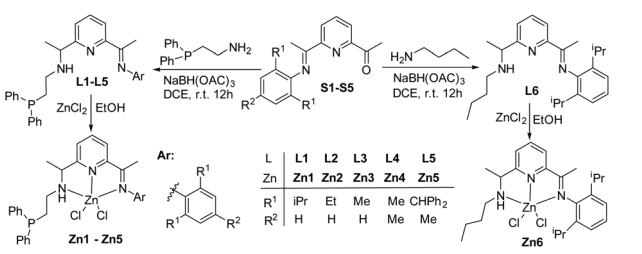

Scheme 1 Synthesis of **L1–L6** and the corresponding zinc(II) chloride complexes **Zn1–Zn6**.

Table 1 The selected bond lengths and bond angles of **Zn1** and **Zn4**

	Zn1	Zn4
Bond lengths (Å)		
Zn1–Cl1	2.245(12)	2.261(7)
Zn1–Cl2	2.233(13)	2.255(7)
Zn1–N1	2.325(3)	2.352(2)
Zn1–N2	2.069(3)	2.069(2)
Zn1–N3	2.282(4)	2.219(2)
N1–C2	1.281(5)	1.279(4)
N3–C8	1.466(8)	1.486(4)
Bond angles (°)		
Cl1–Zn1–N1	95.80(8)	91.14(6)
Cl1–Zn1–N3	95.17(13)	97.61(7)
Cl2–Zn1–Cl1	120.92(5)	118.29(3)
Cl2–Zn1–N1	102.62(8)	102.86(6)
Cl2–Zn1–N3	95.58(14)	99.42(6)
N2–Zn1–Cl1	117.97(10)	125.42(7)
N2–Zn1–Cl2	121.01(11)	116.15(7)
N2–Zn1–N1	74.05(13)	73.27(9)
N2–Zn1–N3	75.99(16)	77.07(9)

of pyridine than N_{imine} and N_{amine}. In both cases, the phosphine donor remains uncoordinated and is remote from the zinc center, which agrees well with the slight shift of their ^{31}P NMR signals, similar to the previous results.[32] Although the different substituents on the aryl in **Zn1** and **Zn4** lead to variation of Zn–N bond length, the Zn–Cl bond lengths are very similar, with a range of [2.2552(7)–2.2606(7) Å].

Ring-opening polymerization of L-LA by Zn1–Zn6/LiN(SiMe$_3$)$_2$

In the first instance, **Zn1** was evaluated for the ROP of L-LA by performing the reaction in toluene at room temperature with 250 molar equivalents of the cyclic ester. However, no conversion to PLLA could be detected under these conditions, which can be attributed to the strength of the Zn–Cl bond. With a view to activating the zinc complex for ROP of lactides, an *in situ* approach was employed, whereby **Zn1** was pre-treated with LiN(SiMe$_3$)$_2$ to form the zinc amide derivatives. Such a pre-activation strategy has been reported by our group and others to be a successful way to generate highly efficient initiators.[32–34,37–39] Indeed, we have shown that by pre-treating a range of zinc(II) chloride complexes with LiN(SiMe$_3$)$_2$, extremely high activities for the ROP of ε-CL were observed.[32] Therefore, in this work, LiN(SiMe$_3$)$_2$ [LiHDMS] was employed as the activator.

At a molar ratio of [LA]/Zn = 250 : 1, when 1 equivalent LiHDMS was used to activate **Zn1**, the obtained catalytic mixture was inactive toward ROP of L-LA. In contrast, **Zn1** + 2LiHDMS exhibited good activity for ROP of L-LA, with 80% conversion in 10 minutes (run 1, Table 2). To explore the reaction between LiHDMS and **Zn1**, the reactions of **Zn1** + *n*LiHDMS (*n* = 1–3) were investigated by using ^1H NMR spectroscopy. The results are shown in Fig. 3. The ^1H NMR spectra showed that a new peak appeared at δ 0.24 ppm when 1 equivalent of LiHDMS was added; when 2 equivalents of LiHDMS were added, a new peak appeared at δ 0.18 ppm; whereas a peak at δ 0.28 ppm, attributed to LiHDMS, appeared when 3 equivalents of LiHDMS were added, which indicated that LiHDMS was in excess of the **Zn1**. Therefore, the ring-opening polymerization of L-LA was systematically investigated by **Zn1** + 2LiHDMS.

Using **Zn1** + 2LiN(SiMe$_3$)$_2$ as a catalyst and BnOH as a co-initiator, the ring-opening polymerization of L-LA was investigated at different temperatures and molar ratios. With the co-initiation of 1 equiv. BnOH, 88% conversion of 250 equivalents L-LA could be observed at 30 °C within 10 minutes (run 2,

Table 2 ROP of L-LA using **Zn1–Zn6** with pre-treatment with 2 equiv. LiN(SiMe$_3$)$_2$[a]

Run	Cat.	LA : Zn : BnOH	*T*/°C	*t*/min	Solvent	Conv.[b]/%	$M_{n(calcd)}$[c]	M_n[d]	M_w/M_n[d]	TOF/h^{-1}
1	**Zn1**	250 : 1 : 0	30	10	Toluene	80	2.89	2.18	2.04	285
2	**Zn1**	250 : 1 : 1	30	10	Toluene	88	3.18	1.86	1.26	1320
3	**Zn1**	250 : 1 : 1	30	20	Toluene	97	3.50	1.91	1.25	727.5
4	**Zn1**	250 : 1 : 2	30	10	Toluene	98	1.76	1.15	1.13	1470
5	**Zn1**	250 : 1 : 5	30	10	Toluene	100	0.72	1.00	1.52	1500
6	**Zn1**	250 : 1 : 1	40	10	Toluene	96	3.47	2.03	1.57	1440
7	**Zn1**	250 : 1 : 1	50	10	Toluene	97	3.50	2.14	1.30	1455
8	**Zn1**	250 : 1 : 1	60	10	Toluene	100	3.61	2.55	1.94	1500
9	**Zn1**	250 : 1 : 1	60	10	Hexane	40	1.45	1.06	1.47	600
10	**Zn1**	250 : 1 : 1	60	10	THF	44	1.60	1.33	1.88	660
11	**Zn1**	250 : 1 : 1	30	10	CH_2Cl_2					
12	**Zn1**	500 : 1 : 1	60	10	Toluene	96	6.92	1.48	1.24	2880
13	**Zn1**	1000 : 1 : 1	60	10	Toluene	73	10.53	1.24	1.71	4380
14	**Zn1**	1000 : 1 : 1	70	10	Toluene	85	12.25	1.83	1.82	5100
15	**Zn1**	1000 : 1 : 1	80	10	Toluene	95	13.69	1.73	1.89	5700
16	**Zn1**	2000 : 1 : 1	80	10	Toluene	58	16.72	1.95	1.86	6960
17	**Zn1**	2000 : 1 : 1	90	10	Toluene	79	22.77	1.91	1.66	9480
18	**Zn1**	2000 : 1 : 1	100	10	Toluene	86	24.79	1.85	1.90	10 320
19	**Zn1**	500 : 1 : 1	60	5	Toluene	76	5.48	1.83	1.74	4560
20	**Zn2**	500 : 1 : 1	60	5	Toluene	61	4.40	1.53	1.61	3660
21	**Zn3**	500 : 1 : 1	60	5	Toluene	53	3.83	1.67	1.18	3180
22	**Zn4**	500 : 1 : 1	60	5	Toluene	62	4.48	1.69	1.24	3720
23	**Zn5**	500 : 1 : 1	60	5	Toluene	64	4.62	2.18	1.25	3840
24	**Zn6**	500 : 1 : 1	60	5	Toluene	41	3.45	1.13	1.16	2880

[a] Reaction conditions: 10 μmol (pre)cat., 1 mL toluene. [b] Determined by ^1H NMR spectroscopy. [c] $M_{n\ (calcd)} = M_{(LA)} \times$ conversion $\times ([LA]_0/[Zn]_0) + M_{BnOH} \times 10^4$ g mol^{-1}. [d] GPC data were recorded in THF *vs.* polystyrene standards using a correction factor of 0.58.[40]

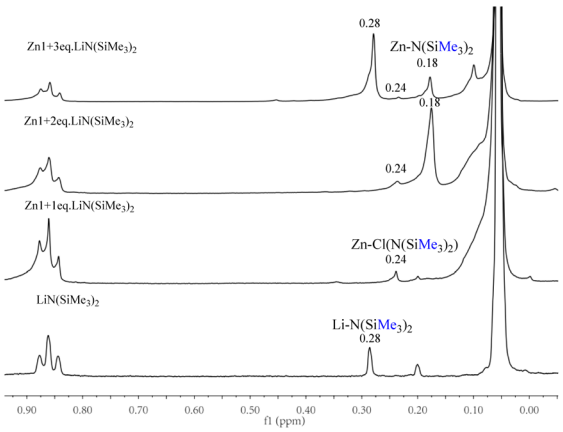

Fig. 3 Comparison of ^{1}H NMR spectra of **Zn1** reacting with different equivalents of LiHDMS *in situ* (in d_8-toluene).

Table 2). In contrast, under the same conditions, without BnOH, the conversion was 80% (run 1, Table 2). When the molar ratio of BnOH was increased to 2 or 5 equivalents, the conversion gradually increased from 88% to 100%, and the M_n of the obtained PLLA rapidly decreased from 2.18×10^4 to 1.00×10^4 g mol^{-1}, clearly suggesting the chain transfer role of BnOH (runs 4 and 5, Table 2).

The temperature also greatly influenced the catalytic activity. When the temperature was increased from 30 °C to 40 °C, the monomer conversion increased from 88% to 96% (run 6, Table 2). Further increasing the temperature to 60 °C led to almost quantitative conversion of L-LA (>96%) (runs 6–8, Table 2). The molecular weight distribution of the polymers obtained at 60 °C was broader (PDI = 1.94), which may be due to increased transesterification at higher temperatures. The solvent also had a great effect on the catalytic activity. When hexane and THF were used as solvents, the activity was almost halved, and the conversion dramatically decreased from 100% to 40% or 44%. No monomer conversion was achieved when CH_2Cl_2 was used as solvent (runs 9–11, Table 2).

Fixing the temperature at 60 °C and the polymerization time at 10 min, when increasing the monomer to metal ratio from 250 to 500 (runs 8, 12, and 13, Table 2), the monomer conversion decreased slightly from 100% to 96% within 10 min, indicating that the system has good catalytic efficiency. Further increasing the monomer-to-zinc molar ratio to 1000 resulted in a lower monomer conversion of 73%. The TOF value increased from 1500 h^{-1} to 4380 h^{-1} when the monomer-to-zinc molar ratio was increased from 250 to 1000 (run 13, Table 2).

At a high molar ratio of [LA] to [Zn] of 1000, elevating the temperature from 60 °C to 80 °C led to a gradual increase in the monomer conversion from 73% to 95%, and the TOF values also increased from 4380 to 5700 h^{-1} (runs 13–15, Table 2). When setting a higher molar ratio of [LA] : [Zn] of 2000 and increasing the temperature from 80 °C to 100 °C within 10 minutes, the TOF values increased from 6960 h^{-1} to 10 320 h^{-1} (runs 16–18, Table 2). At these high molar ratios of monomer to zinc, although the TOF values are high, the molecular weight M_n of the polymer (ranging from 1.24 to 1.95×10^4 g mol^{-1}) is much lower than the theoretical molecular weight ($10.51–22.77 \times 10^4$ g mol^{-1}). Meanwhile, the molecular weight distribution is also broad, with PDI = 1.66–1.90. These results suggest that more transesterification side reactions occur at high molar ratios and high temperature in the polymerization.

Since **Zn1** + 2LiN(SiMe$_3$)$_2$ can efficiently catalyze the ring-opening polymerization in the presence of BnOH, as demonstrated by 96% conversion at 500 equivalents of monomer at 60 °C within 10 min, the ring-opening polymerization performance of complexes **Zn1–Zn6** with 2 equiv. LiN(SiMe$_3$)$_2$ were investigated individually at 60 °C for 5 min (runs 19–24, Table 2). The results showed *ortho*-substituents on the aryl had a strong influence on the catalytic activity, which was demonstrated by **Zn1** (76%, R^1 = ^{i}Pr) > **Zn2** (61%, R^1 = Et) > **Zn3** (53%, R^1 = Me); whereas the introduction of a *para*-methyl group slightly increased the monomer conversion, with **Zn4** (62%, R^2 = Me) > **Zn3** (53%, R^2 = H).

The molecular weight of the PLLA generated by sterically hindered **Zn5** was relatively high (2.18×10^4 g mol^{-1}), probably due to the high ligand bulk preventing chain transfer. Fig. 4 clearly shows that the phosphorus-free **Zn6** exhibited lower activity than all the other phosphorus-containing complexes **Zn1–Zn5** under the same conditions, with a much lower conversion of 41% than that obtained with other complexes (53%–76%). In particular, the molecular weight of polymers obtained by **Zn6** (1.13×10^4 g mol^{-1}) was much lower than that of the polymers obtained from the other complexes ($1.53–2.18 \times 10^4$ g mol^{-1}). Although the crystal structure of **Zn2** and **Zn4** shows that –PPh$_2$ was not involved in coordination because the phosphorus atom is a soft electron donor and its coordination with metallic zinc is weak, the above-mentioned results indicate the important role of phosphorus, which is likely to be involved in coordination during the polymerization process. Both the catalytic activity and the molecular weights of the polymers obtained by **Zn6** are considerably lower than those of the phosphorus-containing complexes **Zn1–Zn5** with similar structures.

A kinetic study with complex **Zn1** was performed for various times in toluene at 60 °C with monomer-to-metal ratios $[LA]_0/[Zn]_0$ of 500 : 1. The $\ln([M]_0/[M]_t)$ was calculated

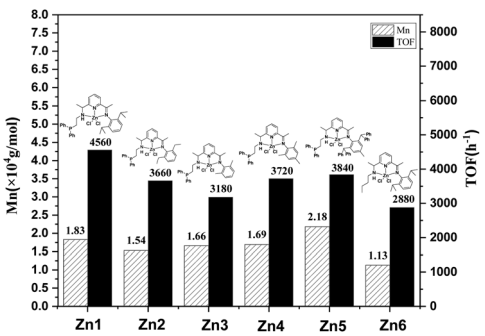

Fig. 4 The substituent effects on the molecular weight of PLLA and TOF values (runs 20–25, Table 2).

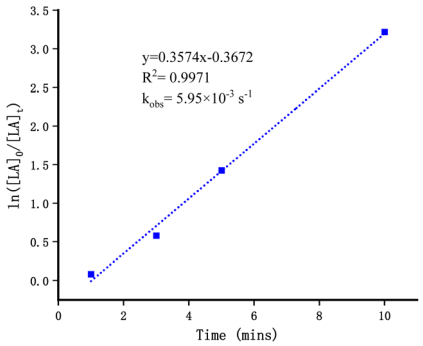

Fig. 5 Kinetic plots for the ROP of L-LA by **Zn1** with [LA]/[Zn]/[BnOH] = 500/1/1 at 60 °C. In toluene.

from the different signals in the ^{1}H NMR spectra from the polymer and the monomer (Fig. 5). The plot of $\ln([M]_0/[M]_t)$ *versus* time was almost linear, showing a first-order dependency of the polymerization rates on the monomer concentration. The apparent rate constants (k_{app}) were calculated from the slope of the observed plots (5.95×10^{-3} s^{-1}).

To clarify the mechanism underlying these polymerizations, the PLLA formed without benzyl alcohol (run 3, Table 2) was characterized *via* MALDI-TOF mass spectrometry and ^{1}H NMR spectroscopy (Fig. 6). The MALDI-TOF mass spectrum of the obtained PLLA exhibits a repeating mass unit of 72 Da, corresponding to half a lactide unit ($C_3H_4O_2$) and indicating the presence of both intermolecular and intramolecular transesterification reactions.

Additionally, the spectrum reveals two distinct peak families: the major set (A/A′/A″) corresponds to cyclic species with the formula $[(C_3H_4O_2)_n + Li^+/Na^+/K^+]$, confirming that the polymer formed in the absence of benzyl alcohol is predominantly cyclic. The minor peaks (B/B′) are attributed to the linear polymer with the structure $[(C_3H_4O_2)_n + CH_3O + Na^+/K^+ + H]$, consistent with methoxy-terminated PLLA. This is further confirmed by the ^{1}H NMR spectrum, which exhibits a small peak at 3.7 ppm corresponding to the methoxy group.

When 1 equivalent of BnOH was added to the polymerization, the MALDI-TOF mass spectrum revealed two families (A/A′/A″ and B). Among these, the family peaks (B) were ascribed to cyclic polymers with the formula $[(C_3H_4O_2)_n + Na^+]$, whereas the intense peaks (A/A′/A″) are attributed to linear polymers with the structure $[(C_3H_4O_2)_n + PhCH_2O + Li^+/Na^+/K^+ + H]$. Consistent with the MALDI-TOF results, the ^{1}H NMR spectrum of PLLA exhibits characteristic signals at 4.43 ppm (PhC*H*$_2$O–) and 7.26 ppm (*Ph*CH$_2$O–) (Fig. 7).

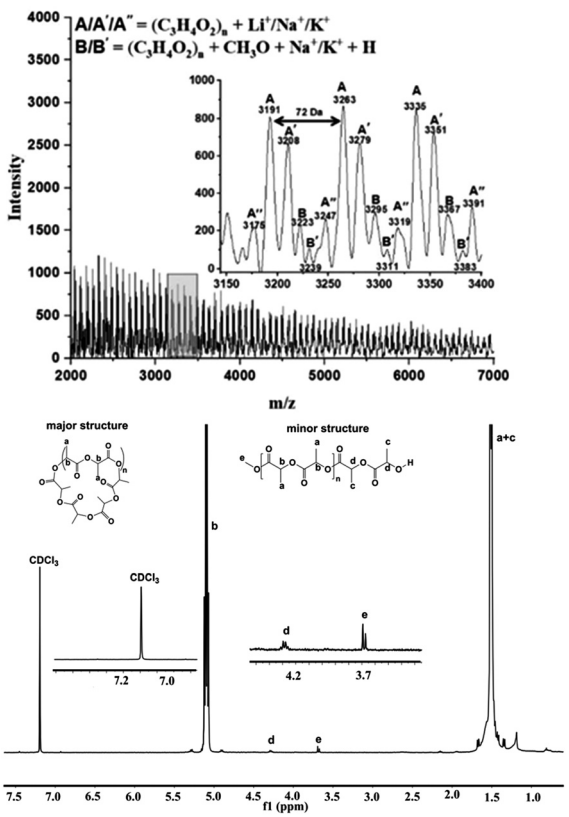

Fig. 6 (Top) MALDI-TOF mass spectrum and ^{1}H NMR spectrum (bottom) recorded in $CDCl_3$ of the obtained PLLA using **Zn1**/2LiN(SiMe$_3$)$_2$ (run 3, Table 2).

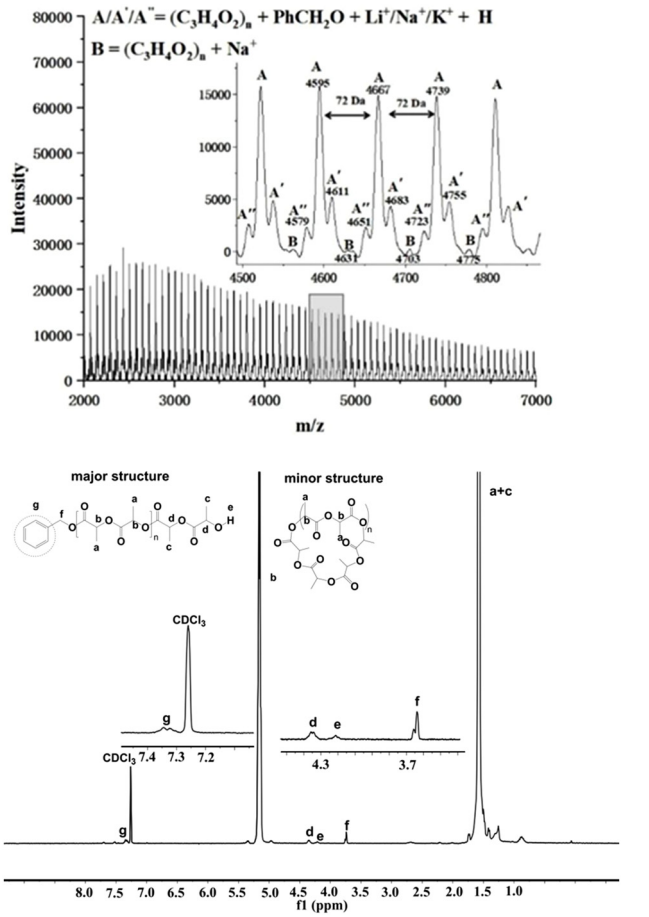

Fig. 7 (Top) MALDI-TOF mass spectrum of the PLLA obtained using **Zn1**/2LiN(SiMe$_3$)$_2$ + 1 eq. BnOH and (bottom) its ^{1}H NMR spectrum recorded in $CDCl_3$ (run 1, Table 2).

When 2 equivalents of benzyl alcohol were used (Fig. 8), the MALDI-TOF mass spectrum of the obtained polymer showed two major families: A/A′/A″ corresponds to polymer chains based on $[(C_3H_4O_2)_n + PhCH_2O + Li^+/Na^+/K^+ + H]$, and B is assignable to cyclic species $[(C_3H_4O_2)_n + Na^+]$. Consistent with the MALDI-TOF results, the ^{1}H NMR spectrum of PLLA in Fig. 8 also exhibits characteristic signals of $PhCH_2O$– at 4.43 ppm and 7.26 ppm. The addition of benzyl alcohol was preferred to produce a linear product capped with a benzyloxy group; however, when the BnOH content was increased further, the ratio of cyclic products also increased, which may be due to the occurrence of chain transfer side reactions, where the resulting polymers are more likely to form cyclic products due to inter-transesterification.

The ring-opening polymerization of L-LA catalyzed by **Zn6** (without phosphorous) was conducted at a monomer ratio of 500 : 1 at 60 °C for 5 min. The conversion was found to be 41%, and the molecular weight of the polymer was 1.13×10^4 g mol^{-1}, which is much lower than that of **Zn1** (76%, 1.83×10^4 g mol^{-1}) under the same conditions, suggesting the positive effect of the phosphorus group in **Zn1**. To gain deeper insights into the role of phosphorus in the polymerization process, the ^{31}P NMR spectra of **Zn1**, **Zn1** + 2 eq. LiHDMS and **Zn1** + 2 eq. LiHDMS + L-LA was measured *in situ* for comparison (shown in Fig. 9). The results showed that the peak in the phosphorus spectrum shifted slightly from −20.94 ppm (**Zn1**) to −20.46 ppm (**Zn1** + 2 eq. LiHDMS), probably due to the change of the Zn–Cl bond to a Zn–N(SiMe$_3$)$_2$ bond. This small shift may be due to dissociation of phosphorus from the zinc. When L-LA was added, two new clear signals appeared at −20.75 ppm and −50.02 ppm, with the latter peak shifting a lot when compared to the original signal, and we speculated that phosphorus atoms might be involved in coordination with zinc to form a new intermediate in the polymerization process. On the basis of the above analysis of the microstructure of the polymer, we propose a mechanism of polymerization as shown in Fig. 10.

Firstly, the absence of –N(SiMe$_3$)$_2$ signals in both ^{1}H NMR and MALDI-TOF spectra suggests that Zn–N(SiMe$_3$)$_2$ is not involved in the initiation of polymerization, which may be related to the large spatial site resistance of this amine com-

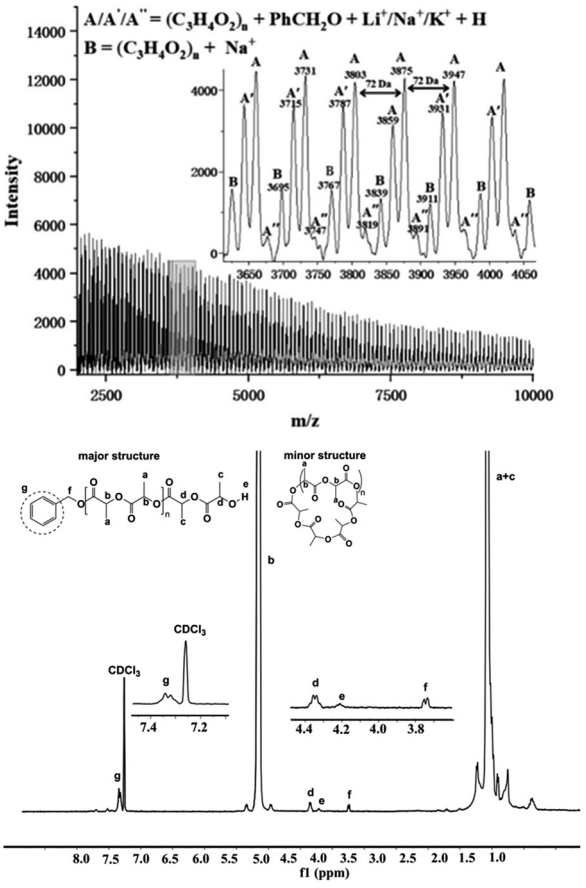

Fig. 8 (Top) MALDI-TOF mass spectrum of the PLLA obtained using **Zn1**/2LiN(SiMe$_3$)$_2$ + 2 eq. BnOH and (bottom) its ^{1}H NMR spectrum recorded in $CDCl_3$ (run 4, Table 2).

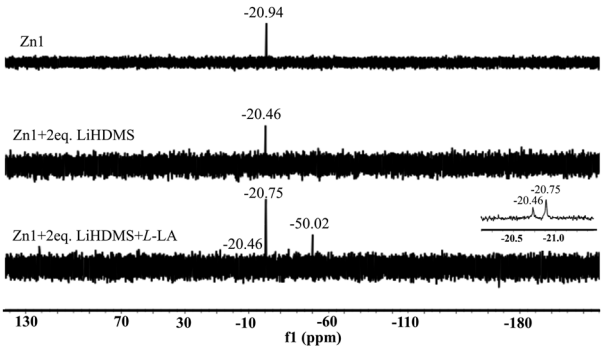

Fig. 9 Comparison of ^{13}P NMR spectra.

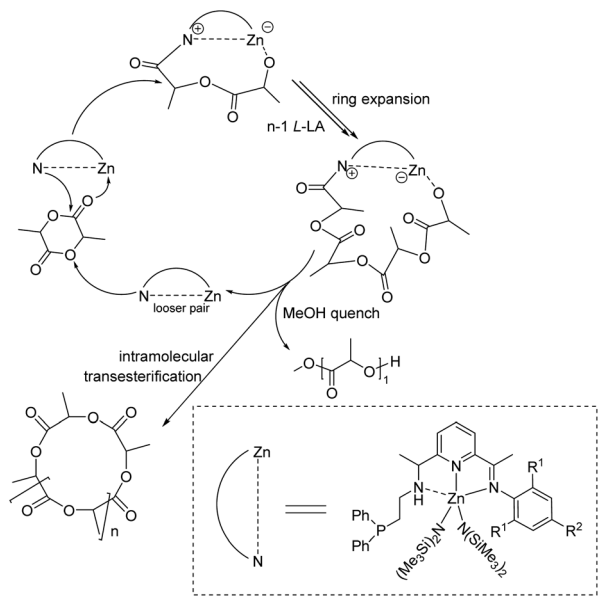

Fig. 10 Possible mechanistic pathways for the ROP of L-LA by **Zn1**/2LiN(SiMe$_3$)$_2$.

Table 3 ROP of *rac*-LA using **Zn1–Zn6** with 2 equiv. $LiN(SiMe_3)_2$[a]

Run	Cat	LA : Zn : BnOH	T/°C	t/min	Conv.[b]/%	$M_{n(calcd)}$[c]	M_n[d]	M_w/M_n[d]	TOF/h^{-1}
1	**Zn1**	500 : 1 : 1	60	5	8	0.59	—	—	480
2	**Zn1**	500 : 1 : 1	70	5	35	2.53	—	—	2100
3	**Zn1**	500 : 1 : 1	80	5	84	6.06	0.42	1.59	5040
4	**Zn2**	500 : 1 : 1	80	5	76	5.48	—	—	4560
5	**Zn3**	500 : 1 : 1	80	5	81	5.84	—	—	4860
6	**Zn4**	500 : 1 : 1	80	5	83	5.99	—	—	4980
7	**Zn5**	500 : 1 : 1	80	5	69	4.98	—	—	4140
8	**Zn6**	500 : 1 : 1	80	5	74	5.34	0.33	1.61	4440

[a] Reaction conditions: 10 μmol (pre)cat., 1 mL toluene. [b] Determined by ^{1}H NMR spectroscopy. [c] $M_{n\ (calcd)} = M_{(LA)} \times$ conversion $\times ([LA]_0/[BnOH]_0) + M_{BnOH} \times 10^4$ g mol^{-1}. [d] GPC data were recorded in THF *vs.* polystyrene standards using a correcting factor of 0.58; "—" not determined.[40]

pound. Based on similar reports in the literature,[41,42] we propose that a Lewis acid–base pair intermediate may be formed, which is 'looser' at higher temperatures and forms an amphiphilic intermediate. This 'loose pair' can initiate the ring-opening polymerization of L-LA that leads to ring expansion followed by formation of an amphoteric intermediate. Thus, this 'loose pair' can trigger the polymerization of L-LA, leading to ring expansion and then the formation of a cyclic macrolactone, and also can be terminated by cold methanol to give a product that is a linear polymer with a methoxy terminal group.[43]

When BnOH was added, the substitution of silylamide by an alkoxide proceeded rapidly, and the resultant zinc alkoxides can act as better initiating groups to generate a polymer with a linear structure and a BnO end group.

Ring-opening polymerization of *rac*-LA by Zn1–Zn6

Ring-opening polymerization of *rac*-LA by **Zn1–Zn6** was also tested, and the results are shown in Table 3. Under the same conditions as the ring-opening polymerization of L-LA (60 °C, 500 equivalents of monomer), the catalyst of **Zn1** + 2 eq. LiHDMS showed low activity, with only 8% monomer conversion in 5 min for the ROP of *rac*-LA, much lower than that (conversion: 76%) for L-LA, and no polymer could be collected. When the temperature was increased from 60 °C to 80 °C, the monomer conversion increased rapidly from 8% to 84% (runs 1–3, Table 3), and the isolated sticky polymer possessed a low molecular weight of 0.42×10^4 g mol^{-1}. Then, the catalytic performance toward ROP of *rac*-LA by different substituted **Zn1–Zn6** was investigated at 80 °C, and the results indicated that the conversion rate varied between 69% and 84%. All the obtained polymers were oily (runs 3–8, Table 3). Considering that the polymers were oily, despite the high conversion of the monomers at higher temperatures, it was proposed that high monomer concentrations might be the result of more side reactions of esterification between the monomers and polymer molecular chains. The results show that all the zinc complexes can catalyze the ring-opening polymerization of *rac*-LA effectively, with TOF values ranging from 4140 h^{-1} to 5040 h^{-1}, but there is no stereoselectivity for the ring-opening polymerization of *rac*-LA. The homonuclear decoupled ^{1}H NMR spectrum of the oily PLA obtained by **Zn4** shows a P_m value of 0.38, consistent with the characteristic microstructure of atactic PLA (shown in SI, Fig. S39).[44] Comparing these results with the results in the literature, these catalysts can be regarded as efficient because most reported efficient catalysts for ring-opening polymerization of L-LA or *rac*-LA have TOF values ranging from 4000 to 6200 h^{-1},[45] and only a few examples show remarkably high TOF values of 60 000 h^{-1}.[22]

Experimental

General considerations

All manipulations were performed under high-purity nitrogen with rigorous exclusion of air and moisture using standard Schlenk techniques or glove boxes. Toluene, *n*-hexane, diethyl ether, and THF were dried over sodium benzophenone under reflux and then distilled under nitrogen and finally stored over activated molecular sieves (4 Å) for 24 h in a glove-box before use. L-LA was purchased from J&K Scientific and used as received. Elemental analysis was carried out with a Flash EA 1112 microanalyzer. ^{1}H and ^{13}C NMR spectra were recorded on a Bruker DMX-400 instrument. The MALDI-TOF spectra were recorded on a Bruker Autoflex III by the linear positive ion method. The GPC measurements were performed using a system composed of a 390-LC Multidetector (MDS), 209-LC pump injection module (PIM), and a PL-GPC 50 plus instrument. THF was used as the eluent (flow rate: 1 mL min^{-1}, at 40 °C), and the molecular weights and molecular weight distributions were calculated using polystyrene as the standard. All reagents were obtained from Aladdin or local suppliers, including DCE (1,2-dichloroethane) from Innochem, THF and toluene from Concord, and diphenylphosphine from Aladdin Incorp. 2,6-Diacetylpyridine was purchased from AstaTech Biopharmaceutical Corp.

Diphenylphosphine ethylamine was prepared according to our previous work.[32] ^{1}H NMR ($CDCl_3$ 400 MHz, TMS): δ 7.44–7.38 (m, 4H), 7.34–7.22 (m, 6H), 2.88–2.76 (m, 2H), 2.22 (m, J = 15.0, 7.4 Hz, 2H), 1.46–1.25 (m, 2H). ^{13}C NMR ($CDCl_3$, 75 MHz, TMS): δ138.3, 138.1, 132.9, 132.6, 129.1, 129.1, 128.9, 128.7, 128.5, 128.4, 39.2, 38.9, 32.2, 32.1. ^{31}P NMR ($CDCl_3$, 162 MHz, TMS): δ −22.40. Different 2-acetyl-6-(arylimino)pyridine compounds were also prepared according to our previous work and called "monoimino compounds".[46]

Synthesis and characterization of L1–L6

Synthesis of 1-(6-(1-((2,6-diisopropylphenyl)imino)ethyl) pyridin-2-yl)-*N*-(2-(diphenylphosphaneyl)ethyl)ethan-1-amine (L1). In a 100 mL Schlenk tube, the diphenylphosphinoethylamine (2.407 g, 10.5 mmol), mono-imino compound **S1** (3.22 g, 10 mmol) and triacetoxy sodium borohydride (2.967 g, 14 mmol) were added, and the reaction system was replaced with a nitrogen atmosphere, 50 mL of dried 1,2-dichloroethane (DCE) was added, and the reaction system was stirred at room temperature for 15 h. The white solid in the reaction system gradually disappeared. After the reaction, the organic layer was quenched with saturated sodium bicarbonate solution (20 mL), and the aqueous layer was extracted with ethyl acetate. The organic layers were combined, the solvent was removed, and the crude product was purified by alumina column chromatography using petroleum ether and ethyl acetate. Yield: 3.39 g, 63%. ^{1}H NMR (400 MHz, $CDCl_3$, TMS): δ 8.21 (d, J = 7.6 Hz, 1H), 7.69 (t, 1H), 7.37 (d, J = 7.1 Hz, 5H), 7.28 (s, 7H), 7.16 (d, J = 7.4 Hz, 2H), 7.12–7.04 (t, 1H), 3.90 (m, J = 12.7, 6.2 Hz, 1H), 2.78–2.73 (m, 2H), 2.67 (d, J = 7.4 Hz, 1H), 2.36–2.24 (m, 2H), 2.20 (s, 3H), 2.10 (s, 1H), 1.42 (s, 3H), 1.15 (d, J = 6.3 Hz, 12H). ^{13}C NMR (101 MHz, $CDCl_3$, TMS): δ 166.22, 162.13, 154.78, 145.54, 137.39, 135.68, 134.73, 131.60, 127.43, 122.43, 121.90, 121.10, 118.22, 76.36, 76.04, 75.72, 57.74, 43.49, 43.29, 28.33, 27.17, 22.21, 21.80, 16.24. ^{31}P NMR (162 MHz, $CDCl_3$, TMS): δ −21.46. Anal. calcd for $C_{35}H_{42}ClN_3P$ (1/10 CH_2Cl_2): C, 77.18; H, 7.77; N, 7.71. Found: C, 77.23; H, 7.93; N, 7.60.

Synthesis of 1-(6-(1-((2,6-diethylphenyl)imino)ethyl)pyridin-2-yl)-*N*-(2-(diphenylphosphaneyl)ethyl)ethan-1-amine (L2). The procedure described for **L1** was used in the preparation of **L2** using diphenylphosphinoethylamine (0.96 g, 4.2 mmol), mono-imino compound **S2** (1.18 g, 4 mmol) and triacetoxy sodium borohydride (1.18 g, 5.6 mmol). A yellow oily product was obtained by basic alumina column chromatography with petroleum ether/ethyl acetate (10/1, v/v). Yield: 1.02 g, 47.59%. ^{1}H NMR (400 MHz, $CDCl_3$, TMS): δ 8.20 (d, J = 7.7 Hz, 1H), 7.74–7.66 (t, 1H), 7.43–7.33 (m, 4H), 7.28 (m, J = 3.9, 2.5 Hz, 6H), 7.11 (d, J = 7.5 Hz, 2H), 7.06–6.99 (t, 1H), 3.89 (m, J = 6.6 Hz, 1H), 2.81–2.56 (m, 2H), 2.47–2.32 (m, 4H), 2.32–2.20 (m, 2H), 2.17 (s, 3H), 1.43–1.39 (t, 3H), 1.13 (m, J = 7.5, 2.6 Hz, 6H). ^{13}C NMR (101 MHz, $CDCl_3$, TMS): δ 166.18, 162.08, 154.79, 146.86, 137.41, 135.68, 131.61, 130.12, 127.39, 124.82, 122.17, 121.13, 118.18, 76.05, 57.79, 43.50, 28.26, 23.54, 21.71, 15.87, 12.68. ^{31}P NMR (162 MHz, $CDCl_3$, TMS): δ −21.31. Anal. calcd for $C_{33}H_{38}N_3P$ (3/10 CH_2Cl_2): C, 75.02; H, 7.30; N, 7.88. Found: C, 74.93; H, 7.58; N, 7.61.

Synthesis of 1-(6-(1-((2,6-dimethylphenyl)imino)ethyl) pyridin-2-yl)-*N*-(2-(diphenylphosphaneyl)ethyl)ethan-1-amine (L3). The procedure described for **L1** was used for the preparation of **L3** using diphenylphosphinoethylamine (2.407 g, 10.5 mmol), mono-imino compound **S3** (2.66 g, 10 mmol) and triacetoxy sodium borohydride (2.967 g, 14 mmol). A yellow oily product was obtained by basic alumina column chromatography with petroleum ether/ethyl acetate (10/1, v/v). Yield: 1.26 g, 26%. ^{1}H NMR (400 MHz, $CDCl_3$, TMS) δ 8.21 (d, J = 7.8 Hz, 1H), 7.70 (t, J = 7.7 Hz, 1H), 7.42–7.33 (m, 4H), 7.28 (d, J = 10.9 Hz, 6H), 7.06 (d, J = 7.4 Hz, 2H), 6.93 (t, J = 7.4 Hz, 1H), 3.89 (m, J = 12.7, 6.1 Hz, 1H), 2.82–2.58 (m, 2H), 2.36–2.22 (m, 2H), 2.16 (s, 3H), 2.04 (s, 6H), 1.40 (d, J = 6.6 Hz, 3H). ^{13}C NMR (101 MHz, $CDCl_3$, TMS): δ 166.49, 162.14, 154.77, 147.81, 137.44, 135.67, 131.61, 127.67, 127.10, 124.37, 121.87, 121.17, 118.22, 57.77, 43.50, 43.29, 25.87, 21.69, 16.90, 15.53. ^{31}P NMR (162 MHz, $CDCl_3$, TMS): δ −21.33. Anal. calcd for $C_{31}H_{34}N_3P$ (1/2 CH_2Cl_2): C, 72.47; H, 6.76; N, 8.05. Found: C, 72.52; H, 7.30; N, 7.76.

Synthesis of 2-(diphenylphosphanyl)-*N*-(1-(6-(1-(mesitylimino)ethyl) pyridin-2-yl)ethyl)ethan-1-amine (L4). The procedure described for **L1** was used in the preparation of **L4** using diphenylphosphino-ethylamine (1.92 g, 8.4 mmol), mono-imino compound **S4** (2.24 g, 8 mmol) and triacetoxy sodium borohydride (2.36 g, 11 mmol). A yellow oily product was obtained by basic alumina column chromatography with petroleum ether/ethyl acetate (10/1, v/v). Yield: 1.57 g, 40%. ^{1}H NMR (400 MHz, $CDCl_3$, TMS): δ 8.19 (d, J = 7.9 Hz, 1H), 7.69 (t, J = 7.9 Hz, 1H), 7.37 (d, J = 4.8 Hz, 4H), 7.29 (s, 7H), 6.88 (s, 2H), 3.89 (d, J = 6.5 Hz, 1H), 2.74–2.64 (m, 2H), 2.29 (s, 3H), 2.15 (s, 3H), 2.00 (s, 6H), 1.39 (d, J = 6.6 Hz, 3H), 1.25 (d, J = 6.3 Hz, 2H). ^{13}C NMR (101 MHz, $CDCl_3$, TMS): δ 166.66, 162.01, 154.89, 145.29, 137.41, 135.65, 131.59, 127.39, 124.19, 121.11, 118.25, 57.71, 43.35, 28.22, 21.69, 19.64, 16.86, 15.53. ^{31}P NMR (162 MHz, $CDCl_3$, TMS): δ −21.29. Anal. calcd for $C_{32}H_{36}N_3P$ (1/2CH_2Cl_2): C, 72.81; H, 6.96; N, 7.84. Found: C, 72.54; H, 7.57; N, 7.69.

Synthesis of 1-(6-(1-((2,6-dibenzhydryl-4-methylphenyl) imino)ethyl) pyridin-2-yl)-*N*-(2(diphenylphosphanyl)ethyl) ethan-1-amine (L5). The procedure described for **L1** was used to prepare **L4** by using diphenylphosphinoethylamine (0.67 g, 2.94 mmol), mono-imino compound **S5** (1.65 g, 2.8 mmol) and triacetoxy sodium borohydride (0.81 g, 3.8 mmol). A yellow oily product was obtained by basic alumina column chromatography with petroleum ether/ethyl acetate (10/1, v/v). Yield: 0.88 g, 38.26%. ^{1}H NMR (400 MHz, $CDCl_3$, TMS): δ 8.16 (d, J = 7.5 Hz, 1H), 8.07 (d, J = 7.6 Hz, 1H), 7.85 (t, J = 7.8 Hz, 1H), 7.19 (m, J = 12.1, 6.5 Hz, 12H), 7.01 (t, J = 6.9 Hz, 8H), 6.69 (s, 2H), 5.25 (s, 2H), 2.66 (s, 3H), 2.18 (s, 3H), 1.08 (s, 3H). ^{13}C NMR (101 MHz, $CDCl_3$, TMS): δ 169.17, 161.73, 154.69, 145.17, 142.75, 141.64, 137.44, 135.44, 131.60, 130.42, 128.87, 128.32, 127.28, 126.95, 125.06, 121.02, 118.27, 57.50, 50.99, 28.31, 25.89, 21.67, 20.29, 15.91. ^{31}P NMR (162 MHz, $CDCl_3$, TMS) δ −21.33. Anal. calcd for $C_{56}H_{52}N_3P$ (4 CH_2Cl_2): C, 63.34; H, 5.32; N, 3.69. Found: C, 63.47; H, 6.96; N, 3.21.

Synthesis of *N*-(1-(6-(1-((2,6-diisopropylphenyl)imino)ethyl) pyridin-2-yl)ethyl)butan-1-amine (L6). The procedure described for **L1** was used in the preparation of **L6** using butan-1-amine (0.76 g, 10.4 mmol), mono-imino compound **1** (3 g, 9.3 mmol) and triacetoxy sodium borohydride (2.97 g, 14 mmol). The yellow oily product was obtained by basic alumina column chromatography with petroleum ether/ethyl acetate (10/1, v/v). Yield: 1.14 g, 32%.^{1}H NMR (400 MHz, $CDCl_3$, TMS): δ 8.20 (d, 1H), 7.75 (t, J = 7.7 Hz, 1H), 7.36 (d, J =

7.6, 0.7 Hz, 1H), 7.16 (d, J = 7.2 Hz, 2H), 7.09 (t, J = 8.5, 6.7 Hz, 1H), 3.91 (q, J = 6.7 Hz, 1H), 2.80–2.70 (m, 2H), 2.63–2.54 (m, 1H), 2.48 (m, J = 11.2, 7.3 Hz, 1H), 2.20 (d, J = 5.2 Hz, 3H), 1.55–1.47 (m, 2H), 1.44 (d, J = 6.7 Hz, 3H), 1.34 (m, J = 11.7, 5.9 Hz, 2H), 1.15 (m, J = 6.9, 2.1 Hz, 12H), 0.88 (t, 3H). ^{13}C NMR (101 MHz, $CDCl_3$, TMS): δ 166.27, 162.58, 154.83, 145.59, 135.66, 134.75, 122.64, 122.04, 121.91, 121.71, 121.09, 118.13, 76.53, 76.10, 76.06, 75.74, 58.07, 46.45, 31.55, 27.20, 27.00, 26.52, 23.38, 22.89, 21.97, 21.41, 19.47, 16.17, 12.91. Anal. calcd for $C_{25}H_{37}N_3$ (1/5 CH_2Cl_2): C, 76.32; H, 9.51; N, 10.60. Found: C, 76.26; H, 9.7; N, 10.47.

Synthesis and characterization of zinc complexes Zn1–Zn6

Synthesis of zinc complex Zn1. In a 100 mL Schlenk tube, 1-(6-(1-((2,6-diisopropylphenyl)imino)ethyl)pyridin-2-yl)-*N*-(2-(diphenyl-phosphaneyl)ethyl)ethan-1-amine (**L1**) (0.535 g,10 mmol) was added to 10 mL ethanol solution and stirred at room temperature until the oil substance was completely dissolved. Zinc chloride (0.136 g, 10 mmol) was dissolved in a 5 mL ethanol solution, and the solution of ligand was added dropwise. The mixture was stirred at room temperature for 12 hours, during which a white solid was produced, which was filtered at the end of the reaction and then washed three times with cold ethanol and dried naturally. A white product was obtained. Yield: 0.53 g, 80%.^{1}H NMR (400 MHz, $CDCl_3$, TMS): δ 8.15 (t, J = 7.8 Hz, 1H), 7.94 (d, J = 7.7 Hz, 1H), 7.62 (d, J = 8.0 Hz, 1H), 7.46 (d, J = 7.7 Hz, 4H), 7.30 (d, J = 7.0 Hz, 6H), 7.22 (s, 3H), 4.13 (s, 1H), 3.31 (s, 1H), 2.98 (s, 2H), 2.60 (s, 2H), 2.37 (s, 1H), 2.31 (s, 3H), 1.61 (d, J = 6.8 Hz, 3H), 1.34 (t, J = 6.4 Hz, 6H), 1.26 (s, 1H), 1.00 (d, J = 6.8 Hz, 6H). ^{13}C NMR (101 MHz, $CDCl_3$, TMS): δ 164.46, 160.88, 145.95, 141.93, 141.11, 138.26, 136.40, 131.83, 128.18, 127.32, 125.10, 122.89, 76.46, 76.14, 75.82, 55.06, 44.16, 43.94, 27.31, 26.61, 24.00, 23.37, 20.15, 17.79. ^{31}P NMR (162 MHz, $CDCl_3$, TMS): δ −20.94. Anal. calcd for $C_{35}H_{42}Cl_2N_3PZn$ (1/10 CH_2Cl_2): C, 61.95; H, 6.25; N, 6.18. Found: C, 61.84; H, 6.30; N, 6.05.

Synthesis of zinc complex Zn2. Zn2 was synthesized using **L2**, according to the aforementioned synthesis of **Zn1**. Yield: 0.43 g, 60%. ^{1}H NMR (400 MHz, $CDCl_3$, TMS): δ 8.05 (d, J = 7.1 Hz, 1H), 7.87 (d, J = 6.9 Hz, 1H), 7.49 (d, J = 6.8 Hz, 1H), 7.43–7.28 (m, 4H), 7.20 (d, J = 10.0 Hz, 7H), 7.04 (s, 3H), 4.02 (s, 1H), 3.18 (s, 1H), 2.89 (d, J = 29.3 Hz, 1H), 2.78 (m, J = 21.7, 7.0 Hz, 2H), 2.52 (s, 2H), 2.27 (s, 2H), 2.13 (s, 3H), 1.48 (d, J = 5.2 Hz, 3H), 1.05 (s, 6H). ^{13}C NMR (101 MHz, $CDCl_3$, TMS): δ 161.09, 146.19, 142.54, 141.55, 132.63, 132.10, 131.70, 127.93, 127.80, 127.32, 124.62, 122.44, 76.36, 76.04, 75.72, 55.15, 44.07, 43.96–43.72, 26.55, 23.04, 20.05, 16.30, 12.77. ^{31}P NMR (162 MHz, $CDCl_3$, TMS): δ −21.47. Anal. calcd for $C_{33}H_{38}Cl_2N_3PZn$ (3/5 CH_2Cl_2): C, 58.08; H, 5.69; N, 6.05. Found: C, 58.15; H, 6.06; N, 5.82.

Zn3 was synthesized using **L3**, according to the aforementioned synthesis of **Zn1**. Yield: 0.38 g, 80%. ^{1}H NMR (400 MHz, $CDCl_3$, TMS): δ 8.13 (t, J = 7.7 Hz, 1H), 7.93 (d, J = 7.3 Hz, 1H), 7.58 (d, J = 7.6 Hz, 1H), 7.51–7.39 (m, 4H), 7.34–7.22 (m, 6H), 7.02 (t, J = 15.6, 6.8 Hz, 3H), 4.11 (s, 1H), 3.26 (s, 1H), 3.00 (s, 1H), 2.60 (s, 2H), 2.39 (s, 1H), 2.22 (s, 3H), 2.20 (s, 6H), 1.58 (s, 3H). ^{13}C NMR (101 MHz, $CDCl_3$, TMS): δ 164.04, 160.92, 146.01, 143.92, 141.79, 136.64, 136.29, 135.77, 131.87, 127.87, 127.87, 127.07, 124.81, 124.36, 122.69, 76.40, 76.08, 75.76, 55.03, 43.97, 26.68, 20.03, 17.96, 15.60. ^{31}P NMR (162 MHz, $CDCl_3$, TMS): δ −21.69. Anal. calcd for $C_{31}H_{34}Cl_2N_3PZn$ (1/5 CH_2Cl_2): C, 59.21; H, 5.48; N, 6.64. Found: C, 58.93; H, 5.68; N, 6.44.

Zn4 was synthesized using **L4**, according to the aforementioned synthesis of **Zn1**. Yield: 0.40 g, 80%. ^{1}H NMR (400 MHz, $CDCl_3$, TMS): δ 8.08 (s, 1H), 7.88 (s, 1H), 7.56 (s, 1H), 7.50–7.34 (m, 4H), 7.23 (d, J = 7.8 Hz, 6H), 6.83 (s, 2H), 4.12 (d, J = 27.8 Hz, 1H), 3.21 (s, 1H), 2.98 (s, 1H), 2.58 (s, 2H), 2.20 (s, 3H), 2.18 (s, 3H), 2.14 (s, 3H), 2.10 (s, 3H), 1.19 (s, 3H). ^{13}C NMR (101 MHz, $CDCl_3$, TMS): δ 141.94, 133.18, 132.77, 129.13, 128.69, 128.33, 127.89, 77.35, 77.03, 76.71, 56.27, 21.60, 21.01, 20.79, 18.90, 16.47, 1.03. ^{31}P NMR (162 MHz, $CDCl_3$, TMS): δ −21.29. Anal. calcd for $C_{32}H_{36}Cl_2N_3PZn$ (3/10 CH_2Cl_2): C, 59.19; H, 5.63; N, 6.41. Found: C, 59.17; H, 5.85; N, 6.23.

Zn5 was synthesized using **L5** according to the aforementioned synthesis of **Zn1**. Yield: 0.35 g, 75%. ^{1}H NMR (400 MHz, $CDCl_3$, TMS): δ 7.95 (t, 1H), 7.56 (d, J = 7.8 Hz, 1H), 7.49 (s, 2H), 7.42 (s, 2H), 7.36–7.27 (m, 6H), 7.21 (s, 6H), 7.13 (d, J = 6.5 Hz, 2H), 7.01 (s, 9H), 6.89 (s, 2H), 6.69 (t, J = 9.4 Hz, 2H), 6.23 (s, 1H), 6.10 (s, 1H), 4.23 (s, 1H), 3.38 (s, 1H), 3.16 (s, 1H), 2.81–2.43 (m, 3H), 2.14 (s, 3H), 1.68 (d, J = 5.3 Hz, 3H), 1.26 (s, 2H).^{13}C NMR (101 MHz, $CDCl_3$, TMS): δ 49.72, 42.04, 27.62, 24.43, 23.39, 22.89, 22.14, 15.83, 14.88, 13.47, 10.81, 10.60, 10.08, 9.65, 8.90, 8.83, 8.33, 6.82, 6.19, 5.87, 2.96. ^{31}P NMR (162 MHz, $CDCl_3$, TMS): δ −21.15. Anal. calcd for $C_{56}H_{52}Cl_2N_3PZn$ (4/5 CH_2Cl_2): C, 68.07; H, 5.39; N, 4.19. Found: C, 59.17; H, 5.72; N, 4.11.

Zn6 was synthesized using **L6**, according to the aforementioned synthesis of **Zn1**. Yield: 0.34 g, 69%. ^{1}H NMR (400 MHz, $CDCl_3$, TMS): δ 8.09 (d, J = 7.3 Hz, 1H), 7.88 (d, J = 7.5 Hz, 1H), 7.59 (s, 1H), 7.18 (d, J = 9.0 Hz, 1H), 4.16 (s, 1H), 3.17–2.95 (m, 2H), 2.93–2.74 (m, 2H), 2.22 (d, J = 14.8 Hz, 3H), 1.64 (d, J = 5.7 Hz, 3H), 1.55 (d, J = 16.0 Hz, 5H), 1.25 (t, J = 18.1 Hz, 9H), 0.95 (d, J = 6.6 Hz, 6H), 0.84 (t, J = 7.2 Hz, 3H).^{13}C NMR (101 MHz, $CDCl_3$, TMS): δ 164.74, 162.45, 147.32, 142.20, 139.16, 126.25, 125.69, 123.94, 123.30, 77.52, 76.90, 76.74, 55.97, 48.08, 30.92, 28.39, 24.96, 24.42, 21.76, 20.32, 18.63, 13.90. Anal. calcd for $C_{25}H_{37}Cl_2N_3Zn$ (1/10 CH_2Cl_2): C, 57.49; H, 7.15; N, 8.01. Found: C, 57.66; H, 7.22; N, 7.94.

General procedure for the ring-opening polymerization of L-LA

The precatalyst **Zn1** (0.0067 g, 0.01 mmol) and toluene (1 mL) were added to a 25 mL Schlenk flask. Then $LiN(SiMe_3)_2$ (2 equivalents) was added dropwise to the solution, and the colour immediately changed from yellow to red-brown. The mixture was then stirred for 30 minutes at room temperature, the sulotion was immediately injected into the L-LA (0.36 g, 2.5 mmol) and then put into the oil bath at a set temperature to react for different times.

Table 4 Crystal data and structure refinements for **Zn1** and **Zn4**

	Zn1	**Zn4**
Empirical formula	$C_{35}H_{41}Cl_2N_3PZn$	$C_{64}H_{72}Cl_4N_6P_2Zn_2$
Formula weight	670.95	1259.75
Temperature/K	169.99(10)	169.99(10)
Crystal system	Monoclinic	Triclinic
Space group	$P2_1/n$	$P\bar{1}$
a/Å	9.03300(10)	14.1106(5)
b/Å	28.6313(4)	15.8409(6)
c/Å	13.76800(10)	16.7144(5)
α/°	90	63.087(4)
β/°	93.0520(10)	69.006(3)
γ/°	90	71.911(3)
Volume/Å^3	3555.72(7)	3060.5(2)
Z	4	2
ρ_{calc}/g cm^{-3}	1.253	1.367
μ/mm^{-1}	2.963	3.407
F(000)	1404	1312
Crystal size/mm^3	0.4 × 0.3 × 0.2	0.1 × 0.08 × 0.03
Radiation	CuKα (λ = 1.54184)	CuKα (λ = 1.54184)
2θ range for data collection/°Index ranges	6.174 to 151.4 $-11 \le h \le 11$ $-35 \le k \le 33$ $-12 \le l \le 17$	6.136 to 151.544 $-17 \le h \le 17$ $-19 \le k \le 17$ $-20 \le l \le 20$
Reflections collected	29 627	43 961
Independent reflections	7156 [R_{int} = 0.0315, R_{sigma} = 0.0273]	12 213 [R_{int} = 0.0433, R_{sigma} = 0.0428]
Data/restraints/parameters	7156/900/666	12 213/272/752
Goodness-of-fit on F^2	1.055	1.031
Final R indexes [$I \ge 2\sigma(I)$]	R_1 = 0.0851 wR_2 = 0.2573	R_1 = 0.0463 wR_2 = 0.1105
Final R indexes [all data]	R_1 = 0.0917 wR_2 = 0.2652	R_1 = 0.0583 wR_2 = 0.1167
Largest diff. peak/hole/e Å^{-3}	0.81/−0.88	1.00/−0.47

Finally, methanol (20 mL) was added to terminate the polymerization, and the resulting polymer was filtered and dried in a vacuum drying oven at 50 °C for 24 h.

X-ray crystallographic studies

Single crystals of **Zn1** and **Zn4** suitable for X-ray structural analysis were grown from a mixture of diethyl ether and dichloromethane at room temperature. The single-crystal X-ray diffraction studies were performed on a Rigaku RAXIS Rapid IP diffractometer with graphite monochromated Cu-Kα radiation (λ = 1.54184 Å) at 170(10) K. Reflections were merged by SHELXL according to the crystal class to calculate the statistics and refinement. Intensities were corrected for Lorentz and polarization effects and empirical absorption. The structures were solved by direct methods and refined by full matrix least-squares on F^2. All non-hydrogen atoms were refined anisotropically. The molecular structures were solved using OLEX2 and refined witih SHELXL program package,[47–49] Crystal data and processing parameters for **Zn1** and **Zn4** are shown in Table 4.[47–49]

Conclusions

A series of pincer-type zinc(II) chloride complexes, **Zn1–Zn6**, bearing unsymmetrical 2,6-bis(arylimino)pyridines (**L1–L6**), has been successfully synthesized in good yields. All the ligands and zinc complexes were fully characterized by ^{1}H/^{13}C/^{31}P NMR spectroscopy as well as elemental analysis. The molecular structures of **Zn1** and **Zn4** revealed a trigonal bipyramid geometry around zinc, with the N-$C_2H_4PPh_2$ arm remaining pendant. By pre-activating **Zn1–Zn6** with two equivalents of LiN(SiMe$_3$)$_2$, the obtained catalysts displayed good activity for ROP of L-LA. At a molar ratio of L-LA : Zn : BnOH of 2000 : 1 : 1, Zn1/2LiN(SiMe$_3$)$_2$ displayed the highest TOF value of 1.03 × 10^4 h^{-1} at 100 °C in 10 minutes. In addition, the **Zn1–Zn6**/2LiN(SiMe$_3$)$_2$ can also effectively catalyse the ring-opening polymerization of *rac*-LA, but their catalytic efficiency is much lower than that for the ROP of L-LA under the same conditions. The phosphorus group played a positive role in ROP of lactides, which was demonstrated by zinc complexes containing the phosphorus group showing higher activity in producing higher molecular weight polymers.

Author contributions

Xiaopan Xue: data curation, investigation; Dongzhi Zhu: data curation; Wenjuan Zhang: conceptualization and writing (equal); Tongxin Zheng: characterization of polymers; Rui Wang: discussion and editing (equal); Yanping Ma: measurement of metal complexes; and Wen-Hua Sun: writing – review and editing (equal).

Conflicts of interest

There are no conflicts to declare.

Data availability

The data supporting this article have been included as part of supplementary information (SI). Supplementary information: ^{1}H/^{13}C/^{31}P NMR spectra of ligand and zinc complexes. CCDC 2506243 (**Zn1**) and 2506244 (**Zn4**) contain the supplementary crystallographic data for this paper.[50a,b] See DOI: https://doi.org/10.1039/d5dt02857d.

Acknowledgements

This work was supported by the National Natural Science Foundation of China (51973005), the Beijing Scholar Program (Project No. RCQJ20303), and the Project of Constructing the Emerging Interdisciplinary Platform Based on "Clothing Science" of the Beijing Institute of Fashion Technology (Classified Development of Municipal Colleges and Universities).

References

1 D. Hubble, S. Nordahl, T. Zhu, N. Baral, C. D. Scown and G. Liu, *ACS Sustainable Chem. Eng.*, 2023, **11**, 8208–8216.

2 A. Stjerndahl, A. F. Wistrand and A.-C. Albertsson, *Biomacromolecules*, 2007, **8**, 937–940.
3 B. N. Mankaev and S. S. Karlov, *Materials*, 2023, **16**, 6682.
4 W. Gruszka and J. A. Garden, *Nat. Commun.*, 2021, **12**, 3252.
5 N. Yadav and T. S. Chundawat, *ChemistrySelect*, 2024, **9**, e202401619.
6 M. J.-L. Tschan, R. M. Gauvin and C. M. Thomas, *Chem. Soc. Rev.*, 2021, **50**, 13587–13608.
7 W. C. Hung, Y. Huang and C. C. Lin, *J. Polym. Sci., Part A: Polym. Chem.*, 2008, **46**, 6466–6476.
8 D. J. Darensbourg and O. Karroonnirun, *Macromolecules*, 2010, **43**, 8880–8886.
9 M. Li, S. Behzadi, M. Chen, W. Pang, F. Wang and C. Tan, *Organometallics*, 2019, **38**, 461–468.
10 D. Zhu, Y. Li, J. Chen and X. Song, *J. Organomet. Chem.*, 2020, **920**, 121317.
11 Y. Yang, H. Wang and H. Ma, *Inorg. Chem.*, 2015, **54**, 5839–5854.
12 C. Fang and H. Ma, *Eur. Polym. J.*, 2019, **119**, 289–297.
13 S. Song, X. Zhang, H. Ma and Y. Yang, *Dalton Trans.*, 2012, **41**, 3266–3277.
14 W.-L. Kong, Z.-Y. Chai and Z.-X. Wang, *Dalton Trans.*, 2014, **43**, 14470–14480.
15 P. M. Schäfer, K. Dankhoff, M. Rothemund, A. N. Ksiazkiewicz, A. Pich, R. Schobert, B. Weber and S. Herres-Pawlis, *Chem. Open*, 2019, **8**, 1020–1026.
16 S. Ghosh, P. M. Schäfer, D. Dittrich, C. Scheiper, P. Steiniger, G. Fink, A. N. Ksiazkiewicz, A. Tjaberings, C. Wölper and A. H. Gröschel, *Chem. Open*, 2019, **8**, 951–960.
17 B. M. Chamberlain, M. Cheng, D. R. Moore, T. M. Ovitt, E. B. Lobkovsky and G. W. Coates, *J. Am. Chem. Soc.*, 2001, **123**, 3229–3238.
18 P. M. Schäfer and S. Herres-Pawlis, *ChemPlusChem*, 2020, **85**, 1044–1052.
19 I. D'Auria, M. C. D'Alterio, C. Tedesco and C. Pellecchia, *RSC Adv.*, 2019, **9**, 32771–32779.
20 G.-J. Chen, S.-X. Zeng, C.-H. Lee, Y.-L. Chang, C.-J. Chang, S. Ding, H.-Y. Chen, K.-H. Wu and I.-J. Chang, *Polymer*, 2020, **194**, 122374.
21 I. D'Auria, V. Ferrara, C. Tedesco, W. Kretschmer, R. Kempe and C. Pellecchia, *ACS Appl. Polym. Mater.*, 2021, **3**, 4035–4043.
22 A. Thevenon, C. Romain, M. S. Bennington, A. J. White, H. J. Davidson, S. Brooker and C. K. Williams, *Angew. Chem., Int. Ed.*, 2016, **55**, 8680–8685.
23 N. Yang, L. Xin, W. Gao, J. Zhang, X. Luo, X. Liu and Y. Mu, *Dalton Trans.*, 2012, **41**, 11454–11463.
24 W.-J. Chuang, H.-Y. Chen, W.-T. Chen, H.-Y. Chang, M. Y. Chiang, H.-Y. Chen and S. C. Hsu, *RSC Adv.*, 2016, **6**, 36705–36714.
25 Y. Han, Q. Feng, Y. Zhang, Y. Zhang and W. Yao, *Polyhedron*, 2017, **121**, 206–210.
26 S. Y. Shaban, *Inorg. Chim. Acta*, 2011, **367**, 212–216.
27 M. Montag and D. Milstein, *Isr. J. Chem.*, 2023, **63**, e202300082.
28 L.-C. Liang, W.-Y. Lee, T.-L. Tsai, Y.-L. Hsu and T.-Y. Lee, *Dalton Trans.*, 2010, **39**, 8748–8758.
29 X.-X. Zheng, C. Zhang and Z.-X. Wang, *J. Organomet. Chem.*, 2015, **783**, 105–115.
30 I. D'Auria, M. Lamberti, M. Mazzeo, S. Milione, G. Roviello and C. Pellecchia, *Chem. – Eur. J.*, 2012, **18**, 2349–2360.
31 I. D'Auria, M. Lamberti, R. Rescigno, V. Venditto and M. Mazzeo, *Heliyon*, 2021, **7**, e07630.
32 F. Cao, Y. Wang, X. Wang, W. Zhang, G. A. Solan, R. Wang, Y. Ma, X. Hao and W.-H. Sun, *Catal. Sci. Technol.*, 2022, **12**, 6687–6703.
33 Y. Wang, W. Zhang, X. Wang, W. Zuo, X. Xue, Y. Ma and W.-H. Sun, *RSC Adv.*, 2023, **13**, 29866–29878.
34 Y. Wang, W. Zhang, P. Zhu, W. You, X. Xue, R. Wang, Y. Ma and W.-H. Sun, *Molecules*, 2024, **29**, 4150.
35 P. Zhu, S. Zhang, W. Zhang, X. Yu, Y. Ma, T. Zheng and W.-H. Sun, *ChemCatChem*, 2025, **17**, e202500083.
36 Z. Wang, G. A. Solan, W. Zhang and W.-H. Sun, *Coord. Chem. Rev.*, 2018, **363**, 92–108.
37 Z. Mou, B. Liu, M. Wang, H. Xie, P. Li, L. Li, S. Li and D. Cui, *Chem. Commun.*, 2014, **50**, 11411–11414.
38 Q. Hu, S.-Y. Jie, P. Braunstein and B.-G. Li, *Chin. J. Polym. Sci.*, 2020, **38**, 240–247.
39 J. Dou, D. Zhu, W. Zhang, R. Wang, S. Wang, Q. Zhang, X. Zhang and W.-H. Sun, *Inorg. Chim. Acta*, 2019, **488**, 299–303.
40 M. Save, M. Schappacher and A. Soum, *Macromol. Chem. Phys.*, 2002, **203**, 889–899.
41 J. A. Castro-Osma, C. Alonso-Moreno, J. C. García-Martinez, J. Fernandez-Baeza, L. F. Sanchez-Barba, A. Lara-Sanchez and A. Otero, *Macromolecules*, 2013, **46**, 6388–6394.
42 N. Maudoux, T. Roisnel, J.-F. Carpentier and Y. Sarazin, *Organometallics*, 2014, **33**, 5740–5748.
43 M. Shaik, J. Peterson and G. Du, *Macromolecules*, 2018, **52**, 157–166.
44 S. S. Roy, S. Sarkar and D. Chakraborty, *Chem. Rec.*, 2021, **21**, 1968–1984.
45 F. Santulli, F. Bruno, M. Mazzeo and M. Lamberti, *ChemCatChem*, 2023, **15**, e202300498.
46 T. Liu, M. Liu, Y. Ma, G. A. Solan, T. Liang and W.-H. Sun, *Eur. J. Inorg. Chem.*, 2022, e202200396.
47 O. V. Dolomanov, L. J. Bourhis, R. J. Gildea, J. A. K. Howard and H. Puschmann, *J. Appl. Crystallogr.*, 2009, **42**, 339–341.
48 G. M. Sheldrick, *Acta Crystallogr., Sect. C:Cryst. Struct. Commun.*, 2015, **71**, 3–8.
49 G. M. Sheldrick, *Acta Crystallogr., Sect. A:Found. Adv.*, 2015, **71**, 3–8.
50 (*a*) CCDC 2506243: Experimental Crystal Structure Determination, 2026, DOI: 10.5517/ccdc.csd.cc2q3ykc; (*b*) CCDC 2506244: Experimental Crystal Structure Determination, 2026, DOI: 10.5517/ccdc.csd.cc2q3yld.